Compression Perception Reconstruction Algorithm for Interferometric Multispectral Image Based on Machine Learning

Shufeng Zhang*

School of Information Engineering, Suzhou Industrial Park Institute of Services Outsourcing, Suzhou 215123, China

Natural signals are generally used in the compressed sensing of multispectral images. However, natural signals do not have sparseness, resulting in the reconstruction time and stability being unable to reach the ideal state. Hence, an interference multispectral image compressed sensing reconstruction algorithm based on machine learning is proposed in this paper. The wavelet transform is used to complete the interference multispectral image coding. The encoded image is used to construct a compressed sensing model. The model is used to find the transformation basis in the natural signal, so that the decomposition coefficients of non-sparse natural signals under this basis are not zero. This solves the problem for non-sparse natural signals. The measurement matrix is designed to ensure the accurate reconstruction of data after effective compression sampling. Then, the SVM decision tree of a machine learning algorithm is used to complete the design of the image reconstruction algorithm. Test results indicate that the proposed algorithm can achieve high stability for both high and low computing platforms. It takes less time and the reconstruction effect is better than that obtained by the existing algorithm. This confirms the usefulness and benefits of the proposed algorithm.

Keywords: multispectral image reconstruction, compressed sensing, machine learning, wavelet transform, transform basis, sparsity

1. INTRODUCTION

In addition to the abundant two-dimensional spatial information obtained from the target, the spectral data also contains one-dimensional spectral information, which is widely used in biomedical, microbial detection, military exploration and other fields (Ramon et al., 2017; Wu et al., 2018; Muggleton et al., 2018). However, with the increase of its spectral dimension, there is a lot of information in the spectral image, and the traditional sampling method is no longer suitable for collecting information from the image. On the other hand, when the optical absorption of the imaging target is weak, the contrasts in the image are reduced, which hampers the analysis of each spectral segment of the target (Nalmpantis and Vrakas, 2019).

*Corresponding Author Email: zhangshufeng335@sina.com

To address the aforementioned problems, researchers have proposed several solutions. At present, the most widely-used spectral reconstruction algorithm involves non-uniform interpolation. This method has several advantages: it is simple and effective; it requires only a small number of calculations; and it can achieve real-time super-resolution reconstruction of multispectral image. However, the interpolation process is too simple and cannot take into account the possible existence of motion estimation and image fusion. Therefore, the reconstruction process has poor stability, and an optimal reconstruction result cannot be guaranteed (Baturay et al., 2017; Fayez et al., 2019; Jia et al. 2019) proposed a Laplacian pyramid-based super-resolution image reconstruction algorithm for a group network. Using group structure as the construction module of the network, there are both forward and feedback connections between the convolution layers.

At the same time, the Laplacian pyramid structure is used to gradually reconstruct a high-resolution image. The results of testing to verify the effectiveness of the algorithm, show that the reconstruction produced by the algorithm is close to the original image, although the computational stability and reconstruction speed is not ideal. Zhan et al. (2019) and Rastogi and Choudhary (2019) proposed a super-resolution image reconstruction algorithm based on image similarity and feature combination is proposed. Firstly, using the cross-scale similarity of image, the KNN algorithm is used to establish the mapping relationship between the pixel features and gradient features of high-resolution and low-resolution images respectively, and then the high-resolution image including high-frequency information is reconstructed by using the mapping relationship between pixel features. Effective high-frequency information is obtained from the input image by using singular value thresholding, and the high-frequency information is amplified and overlaid on the high-resolution image by using the gradient feature mapping relationship, and the final image reconstruction result is obtained. Taking the image segmentation database of the University of California as the experimental data, the experimental results are displayed in MATLAB software under Windows 7. The experimental results show that the details of the reconstructed image are significantly enhanced and the visual effect is greatly improved, although the reconstruction process takes a long time and does not have real-time performance.

In order to solve the aforementioned problems, this paper examines the compression sampling and accurate reconstruction of multispectral image based on the compression sensing and image reconstruction methods. The multispectral image compression and sensing framework based on partially-coherent illumination improves the image contrast and samples the spectral data at a sampling frequency far lower than Nyquist frequency, which solves the problem of spectral image reconstruction.

2. DESIGN OF COMPRESSION PERCEPTION RECONSTRUCTION ALGORITHM OF INTERFEROMETRIC MULTI-SPECTRAL IMAGE BASED ON MACHINE LEARNING

In regard to the spectral imaging of a microorganism, due to its own structural characteristics, the absorption capacity of a microorganism is poor, which leads to the lack of details or even no display. Therefore, in this paper, machine learning technology is used to selectively illuminate the reconstructed object to increase its contrast; also, it uses the principle of compressed sensing, takes image information as a prior condition, and uses the effective wavelet transform method to reconstruct the original spectral data from the compressed low-dimensional data (Guo, 2021).

The theory of compression sensing involves the use of a spatial light modulator to compress the measured image and reconstruct the original data from the compressed low-dimensional data. The theoretical model of compressed

sensing is included in the spectral imaging technology used for microscopic matter. On the basis of the compression sensing measurement model, the separation and compression of the spectral dimension are increased by using the spectral separation device, and the original spectral data is recovered from the low-dimensional measurement value, so as to realize the compression and measurement of the multispectral image. Based on machine learning, the design flow of the interference multispectral image compression and perception reconstruction algorithm is depicted in Figure 1.

The entire design process of this algorithm follows the steps outlined above.

2.1 Wavelet Transform is Used to Complete Interference Multispectral Image Coding

In the design of the reconstruction algorithm, in order to simplify the calculation process, the internal structure and elements of the multispectral image are encoded first. For image coding, wavelet transform technology can effectively improve the speed of image processing. A typical example of the success of wavelet transform in image coding is the embedded bit plane coding based on wavelet. Basically, it sorts the wavelet coefficients according to their contribution to the restored image quality, codes the bit plane one by one, and terminates the coding at any time according to the target code rate or distortion (Cao and Wen, 2019; Bazulin and Sokolov, 2019). Similarly, for a given bitstream, the decoder can end the decoding at any time, and can obtain the recovered image at the corresponding bitstream truncation, so the embedded coding can realize the gradual transmission and gradual emergence of the image, and the rate control is simple.

In order to improve the coding efficiency, the static image sequence coding first encodes an image normally, then creates a template of the recovered image template, and then the subsequent images are matched with the template, and the difference image is encoded. If the correlation between images is strong, good results will be achieved (Awasthi et al., 2018; Jung, 2017). Using the wavelet method for matching can effectively reduce the influence of spectral distribution on image matching and improve the coding efficiency of error image. In the process of setting the encoding, the purpose of quantization is to reduce the entropy of the transform coefficient as much as possible so as to achieve greater compression efficiency in the later stage of coding. However, the distortion caused by the quantization process will directly affect the quality of the restored image after inversion. Therefore, the mean square error criterion which is consistent with the subjective vision is generally used to measure the distortion degree of the restored image, and guide the coding (Akagi et al., 2019).

Set the reconstructed image to have complete and incomplete images. Assume that there is a strong correlation between the two images and they have translation characteristics in space; that is to say, the following relationships exist between the pixel points of the two images:
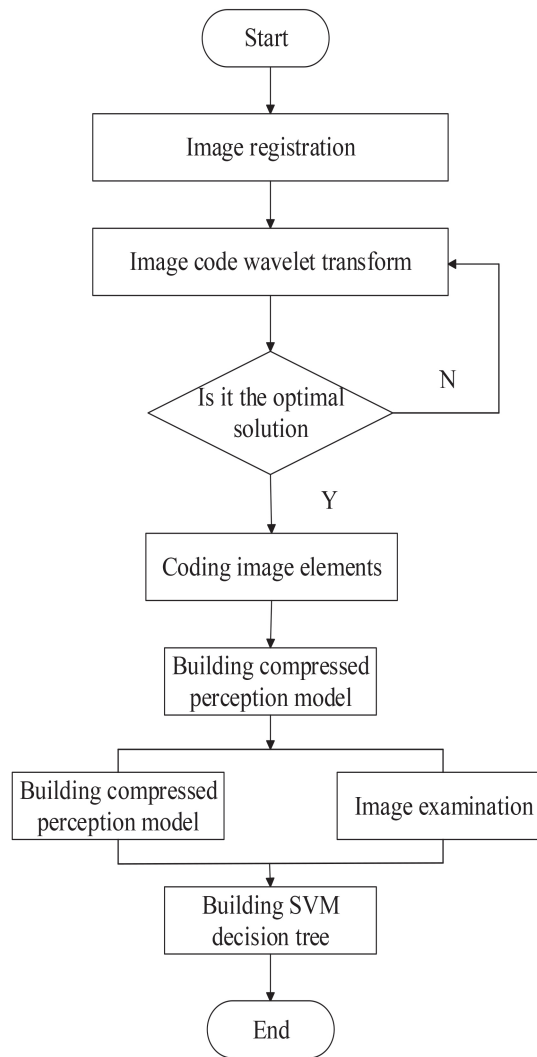
Figure 1 Design flow of algorithm for compression perception reconstruction based on machine learning.

$$a_2(x, y) = \begin{cases} m_1(x + e, y + f) + \Delta m(x, y) \\ m_2(x, y) \end{cases} \quad (1)$$

where, $0 \leq x < C - c$ and $0 \leq y < D - d$. C and D represent the height and width of the image respectively. $m_1(x, y)$ and $m_2(x, y)$ are the pixel values of the image of the complete part and the incomplete part at coordinate (x, y), $\Delta m(x, y)$ is the pixel value of the image at the point of breakage. In order to make full use of the correlation between images and improve the coding efficiency, $m_2(x, y)$ is shifted periodically

$$m_2(x, y) = m_2(x_1, y_1) - [m_2(1 - x) \mod (C), \\ (y - n) \mod (N)] \quad (2)$$

where, mod () represents modular operation. Substituting Equation (2) into Equation (1), the following equation is obtained:

$$m_2(x, y) = m_1(x, y) + \Delta m(x - e, y - f) = m_1(x, y) + \Delta(x, y) \quad (3)$$

where, $\Delta(x, y) = \Delta m(x - e, y - f)$, for $m_1(x, y)$ and $m_2(x, y)$, the sub-band coefficients $n_1(t, u)$ and $n_2(t, u)$ are obtained by the first level wavelet transform, then the following equation is obtained:

$$n_1(t, u) = \sum_{x,y} r_1(t) r_2(u) m_1(x - 2t, y - 2u) \quad (4)$$

$$n_2(t, u) = \sum_{x,y} r_1(t) r_2(u) m_2(x - 2t, y - 2u)$$

$$= \sum_{x,y} r_1(t) r_2(u) m_1(x - 2t, y - 2u)$$

$$+ \sum_{x,y} r_1(t) r_2(u) \Delta m(x - 2t, y - 2u)$$

$$= n_1(t, u) + \Delta(t, u) \quad (5)$$

where (t, u) represents the corresponding coordinates of the coefficients in the wavelet domain, and $r_1(t)$ is the wavelet filter coefficient used in the horizontal and vertical wavelet transform of the sub-band.

In addition to several coefficients at the boundary, substituting Equation (1) into Equation (5), n_2 can be expressed as:

$$n_2(t, u) = \sum_{x,y} r_1(t) r_2(u) m_1(x + c - 2t, y + d - 2u)$$

$$+ \sum_{x,y} r_1(t) r_2(u) \Delta m(x - 2t, y - 2u)$$
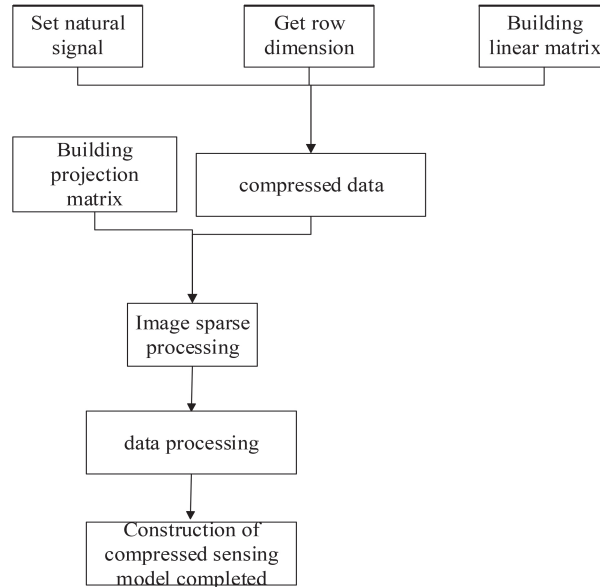
Figure 2 Construction process of compressed perception model.

$$= \sum_{x,y} r_1(t)r_2(u)m_1(x + c - 2t, y + d - 2u)$$
$$+ \Delta n(t, u) \tag{6}$$

where $\Delta(t, u) = \sum_{x,y} r_1(t)r_2(u)\Delta m(x - 2t, y - 2u)$. When c and d are all even, $\Delta n(t, u)$ can be expressed as:

$$\Delta n(t, u) = n_1(t - c/2, u - d/2) + \Delta(t, u) \tag{7}$$

If c and d are odd numbers, Equation (7) does not hold. Although both $n_2(t, u)$ and $n_1(t, u)$ theoretically contain all the information of $m_2(x_1, y_1)$, but $n_1(t, u)$ introduces additional errors relative to $n_2(t, u)$, this is due to the sampling of the coefficients generated in wavelet transform, which is caused by the use of different starting points in wavelet transform. This additional error will be transmitted to the difference image, which is not conducive to the difference image coding.

In order to solve the above problems, Equations (4) and (5) are used to carry out the wavelet transform on the subsequent images to obtain the coefficients. In this step, no additional error will be introduced, which is conducive to the compression of the difference image. The wavelet transform of the difference image is as follows:

$$\Delta n_2(t, u) = n_2(t, u) - n_1(t, u) + \Delta(t, u) \tag{8}$$

The wavelet transform method and the above equations are used to complete the image coding. As the offset between the two images increases, the correlation between the sub-band coefficients will be weakened, and the coefficient correlation differences of different sub-bands will also be larger (Wu et al., 2017; Wen et al., 2019). The coefficients of sub-band 1 represent the high frequency information in the horizontal and vertical directions, which are easily affected by various interference factors, so they are not suitable for matching. The coefficients of sub-band 2 represent the horizontal and vertical low-frequency information and are suitable for image matching. Because the coding technology based on wavelet

transform mainly realizes compression by the high frequency sub-band coefficient, the coefficient of difference image in corresponding sub-band directly affects the coding efficiency. When the corresponding coefficient of difference is large, the compression efficiency cannot be improved by using the difference image, so it is unnecessary to compress the difference image. Therefore, we need to calculate the correlation coefficient of the sub-band coefficient. Only when it meets the preset threshold can the value image be used for encoding, otherwise the image is directly encoded.

2.2 Build Compressed Perception Model

In order to obtain a more suitable reconstruction method for the interference multispectral image, based on the results of interference multispectral image coding, the partially coherent light is innovated and optimized. This is done from a simple (partially coherent) light source (with only one partial coherence factor) to a complex (partially coherent) light source (with internal and external coherence factors). Using the form of constructing the compressed sensing model to complete the image reconstruction, the specific research structure of the compressed sensing model is set as shown in Figure 2.

Following the process above, the image after the coding is adopted. Because a single signal in the image is a one-dimensional natural signal, $z \in S^n$ represents the dimension of the natural signal line, and z^n represents its form, where, $n = 1, 2, 3, \ldots, n$, then $z(n)$ can be expressed by a linear matrix, that is:

$$G = \wp, z - \Delta n_2(t, u) \tag{9}$$

where, linear matrix $\wp$ is a two-dimensional matrix, dimension is $j * k$, and $j < k$. It can be seen from Equation (9) that it is a dimension reduction result of natural signal G projected in the matrix, with dimension $j * 1$. Since the dimension of compressed data G is much smaller than

that of the original data Z, the solution of original signal Z in Equation (9) will become uncertain. The equation will produce infinite solutions. When the original signal itself has sparsity, the original signal can be reconstructed from the compressed measurement signal O by using the solution l optimization problem to realize the signal restoration. The equation is:

$$\bar{z} = \arg \min |z|_0 \qquad (10)$$

where, $|z|_0$ is the norm of the original signal, used to measure the number of non-zero elements in the original signal. According to the theory of compressed sensing, if we want to reconstruct the original signal accurately from the data, then the number of measurements (the number of columns of measurement k) j must be $j = o(\lg(n))$, and the projection matrix $\wp$ satisfies RIP condition, that is:

$$(1 - \Re)|z|_2^2 \le |\wp z|_2^2 \le (1 + \Re)|z|_2^2 \qquad (11)$$

where, $\Re$ constant and $\Re \in (0, 1)$. It can be seen from Equation (11) that the RIP condition ensures that the energy of measured value O after compression is close to the energy of original signal Z. The premise of compressed sensing theory is based on the sparseness of a signal. In the actual environment, natural signal is often not sparse and cannot be applied to compressed reconstruction. Therefore, by using another natural signal property, that is, by finding a set of transformation bases, the decomposition coefficients of non-sparse natural signals under the transformation bases are mostly zero except for a small part which is not zero, that is:

$$z = \sum_{i=1}^{n} \Im_i \aleph_i = \Im \aleph \qquad (12)$$

where, $\aleph_i \in R^{|z|}$ is the decomposition coefficient, $\aleph = |\aleph_1, \aleph_2, \aleph_3, \dots, \aleph_n|$, $\Im_i \in R^{n+1}$ is the transformation basis, $\Im = |\Im_1, \Im_2, \Im_3, \dots, \Im_n|$. $\Im$ is the representation of Z in another field, and its relation is equivalent. The sparse representation of non-sparse signal Z is substituted in the measurement process based on compression perception, as follows:

$$o = \wp z - \wp \Im \Re \cdot R \Im \qquad (13)$$

where, $A \in R^{j*k}$ is a new perception matrix, if A also meets RIP conditions, the coefficient β can be solved by solving the l norm minimum optimization problem of the sparse coefficient of the original signal, that is:

$$\beta = \arg \min |\wp|_0 \qquad (14)$$

The original non-sparse signal is obtained by linear combination of $\Im$ and transform basis $\Re$. In the theory of compressed sensing, in addition to the sparse expression of coefficients, a measurement matrix should also be designed to ensure that the data can be accurately reconstructed after effective compressed sampling. The premise of accurate data recovery is that the signal structure observed by the measurement matrix should be as consistent as possible with the original signal structure. If the measurement matrix destroys the structural information of the original data, the reconstructed signal will be greatly distorted. Therefore, the construction of an ideal measurement matrix is very important for accurate image reconstruction.

In the theory of compressed sensing, the design and construction of the measurement matrix has two aspects according to the sparsity of the original signal. First, when the signal is sparse, there is a problem in the design of the measurement matrix, such as the test matrix δ in Equation (9). According to the above analysis, the natural signal is not sparse in most cases, so it is decomposed into a set of transform basis ϕ and corresponding sparse coefficient ϕ by sparse representation of the signal. After the linear projection of the transformation base under the measurement matrix δ, a new measurement matrix $P = \delta \varphi$ is obtained, known as the compressed sensing matrix, which makes the reconstruction of the signal become a problem when solving the sparse coefficient. In order to accurately reconstruct the sparse coefficient, the compressed sensing matrix P also needs to meet RIP conditions, that is:

$$(1 - \delta)|\varphi|_2^2 \le \beta |P\varphi|_2^2 \le (1 + \delta)|\varphi|_2^2 \qquad (15)$$

According to the RIP property, the compressed sensing matrix P satisfying the condition is approximately orthogonal. RIP condition keeps the distance between the measured signal and the original signal in a very small range, and ensures that the measured signal energy is as close as possible to the original data, so as to improve the accuracy of the reconstructed data. Generally, the distance equation uses the Euclidean distance as a measurement. Following the above steps, the construction of an image compression perception model is completed.

2.3 Using Machine Learning Algorithm to Complete Image Reconstruction Algorithm Design

The interference multispectral image compression and perception reconstruction, according to its composition, involves three stages: data acquisition, data processing and data imaging (Petersen et al., 2018; Min et al., 2019). In order to obtain better image results we use image processing results from data acquisition and data processing to reference the SVM decision tree in the machine learning algorithm to complete the design of image reconstruction algorithm. The steps are as follows:

Data acquisition: Selection of complete image training set (*Train*) and missing image test set (*test*).

The software simulation package is used to simulate the image data with different phase numbers to obtain the data set $Data = \{(m_i, n_i), i = 1, \dots, N\}$, where, N represents the total number of sample sets, in which the data of different phases is recorded as $Data^t = \{m_i^t, n_i^t, i = 1, \dots, N^k, \dots, M\}$, among them, M indicates the presence of no more than M substances in the tube, and N^k represents the number of samples k phase substances. *Data* is divided into training set $Train = \sum_{i=1}^{k} \sum_{j=1}^{n} Data^t$ and test set $test = Data - Train$.

Table 1 Parameters of experimental data set.

Dataset number	Number of images	data dimension
1	2000	8
2	2000	4
3	2000	12
4	2000	6
5	2000	8
6	2000	4

The adaptive prediction model of phase number k based on the SVM decision tree is established for the *Train* sample. According to the different phase number k, the *Train* data is classified and the training set *Train* after classification is obtained; $train^i$ represents the training set sample with phase i material in the predicted tube.

The data obtained above are preprocessed. When the image parameters are determined, the multi-weight normalization model $l_n = \frac{l_i - l^r}{l^M - l^r}$ is used to normalize sample $train^i$ to obtain the training set (*Train'*) and test set (*test'*) after data preprocessing.

Multispectral image reconstruction is a multi-classification problem. The gray level of different media is used as the label of samples for training modeling. Set the training set *Train*, after data preprocessing as $\{(\bar{m}_i, n_i)\}_{i=1}^n$, select the appropriate kernel function $k(\bar{m}_i, m_i)$ and the appropriate parameter l, construct and solve the optimization problem:

$$\max_{\alpha} \sum_{i=1}^{N} \bar{\alpha}_i - \frac{1}{2} \sum_{i=1}^{N} \sum_{i=1}^{N} \bar{\alpha}_i \bar{\alpha}_j n_i n_j k(\bar{m}_i, \bar{n}_i) \left(\beta | P\varphi |_2^2 \right) \quad (16)$$

$$s.t \sum_{i=1}^{N} \bar{\alpha}_i n_i = 0 \quad (17)$$

where, $0 \leq \bar{\alpha}_i \leq l$. Equation (17) obtains the were optimal solution $\bar{\alpha}^t = (\bar{\alpha}_i^t, \ldots, \bar{\alpha}_n^t)^T$. Using this result, the image reconstruction equation is as follows:

$$f(\bar{m}) = \text{sgn} \left[\sum_{i=1}^{N} \bar{\alpha}_i n_i k(\bar{m}, m_i) + b \right] \quad (18)$$

In Equation (18) above, b is a specific point in the image. Equation (18) has been established to integrate the data calculation and realize the reconstruction of the multispectral image. At this point, the design of machine-learning-based interference multispectral image compression and perception reconstruction algorithm is completed.

3. EXAMPLE TEST

In order to verify the reconstruction performance of the interference multispectral image compression and perception reconstruction algorithm based on machine learning proposed in this paper, the corresponding test image is set in this section for reconstruction experiments (Ren, 2021). In this section, the algorithm designed in this paper will be compared with the algorithms in Cao and Wen (2019), Fayez et al., (2019) and Jia et al., (2019).

3.1 Experimental Data and Environment Settings

The images used in the experiment are all from the ImageNet database, which is the largest known image database at present, and comprises numerous kinds of images. 12000 images of different types are selected from the database to form five data sets, including animals, plants, buildings, etc. The data set parameters are shown in Table 1.

Load the above data to the virtual platform. The specific parameters of the platform are: CPU Intel i9, 3.75GHz; Hard disk 1TB solid-state drive; Graphics card AMD; Memory 4G; Operating system Windows 8.

3.2 Test Process

In the experiment, the high-resolution training images in the test system are used as the training set, and these images do not contain any non-multispectral elements. The image in the training data is set to 200mm * 200mm. The original algorithm and the design algorithm are used to reconstruct the missing part of the training set image. In this experiment, the reconstruction speed and stability of the algorithm are compared and displayed as an image. In order to ensure the effectiveness of this test, the testing is conducted on both high- and low-computing platforms to better determine the effectiveness of different algorithms.

3.3 Test Sample

In this test, four images are selected from the training set as the sample. The specific image is shown in Figure 3.

Using the image as the test sample, the image is reconstructed by the design algorithm and the original algorithm, and the test results are obtained and analyzed.

3.4 Experimental Results

3.4.1 Experimental Results for High-Computing-Power Platform

According to the above experimental results, as shown in Figure 4(a), the higher the stability value of image reconstruction using numerical representation, the better the stability. When the calculation level of the test equipment is high, the stability of the four algorithms in the test shows a

(a)

(b)

(c)

(d)
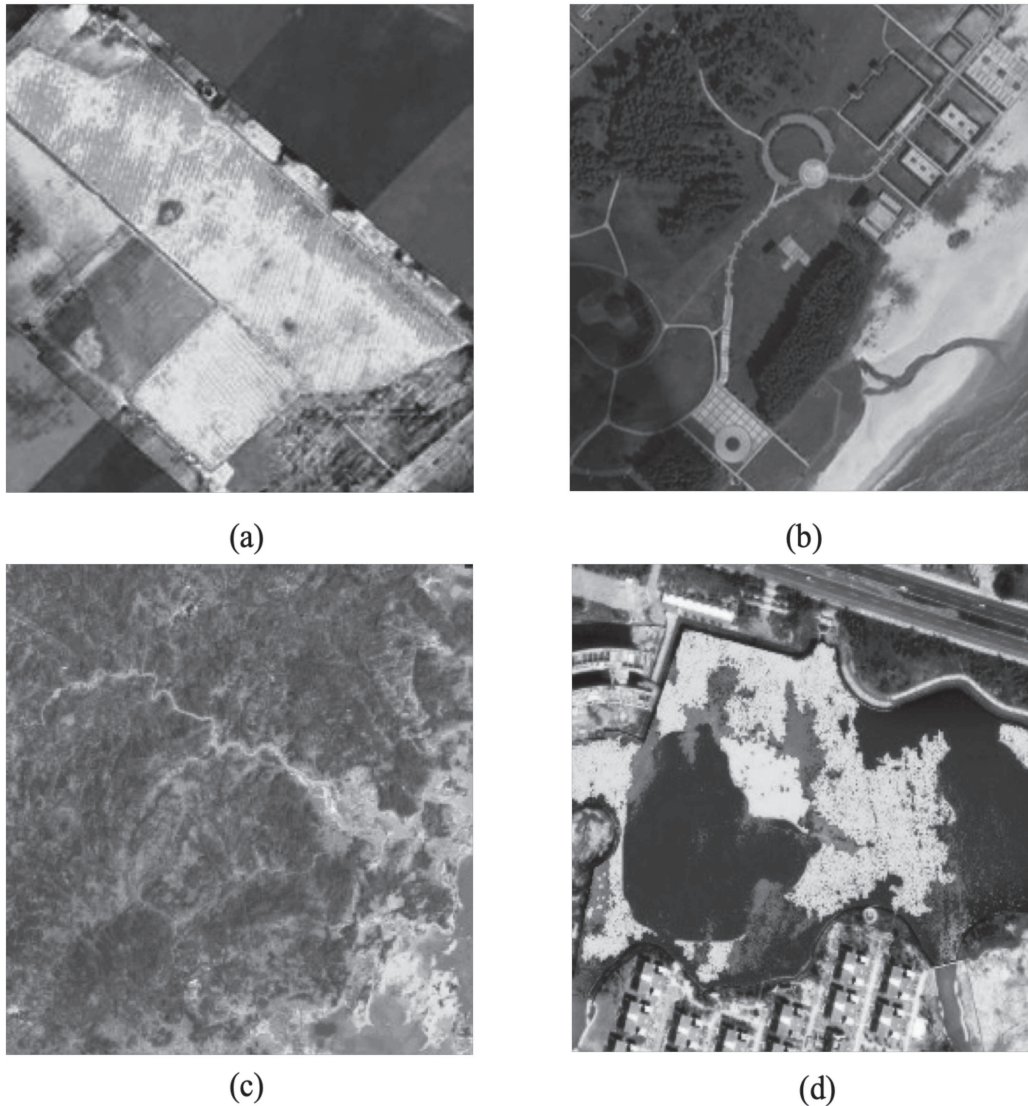
Figure 3 Test sample.

gradual upward trend. The stability of the algorithm designed in this paper is relatively high, the highest value of the stability coefficient reaches 5, and the stability of the algorithm directly reflects the function and effect of the algorithm being applied. It can be seen that the algorithm designed in this study performs better than the original algorithm. In terms of the reconstruction time, the algorithm designed in this paper achieves the shortest construction time compared with that of the other four algorithms, and is always below 1.6 s. It can be seen that the stability and reconstruction speed of the algorithm designed in this paper are the best of the four algorithms when the power of the computing equipment is high.

3.4.2 Experimental Results for Low-Computing-Power Platform

According to the experimental results, when the calculation power of the test equipment is low, of the four algorithms tested, the algorithm (Baturay et al., 2017) and the algorithm (Zhan et al., 2019) are the most affected, and their stability

coefficient fluctuates. Although the algorithm (Jia et al., 2019) has little change, its stability coefficient is still far lower than the algorithm designed in this paper, which is relatively stable. When comparing reconstruction times, the designed algorithm requires the shortest amount of time. Therefore, when the power of the computing equipment is high, the stability and reconstruction speed of the designed algorithm are still better than the other tested algorithms.

The results of the two experiments demonstrate that the algorithm designed in this paper can achieve better results in both high-performance and low-performance platforms. This is because, in order to simplify the calculation process, the internal structure and elements of a multispectral image are encoded first. In the process of image coding, wavelet transform technology can effectively improve the speed of image processing, thus reducing the time required for image reconstruction. At the same time, it takes into consideration that in the actual environment, natural signals are often not sparse and there not suitable for compression and reconstruction. Therefore, by using another property of natural signal, that is, by finding a set of transformation bases,
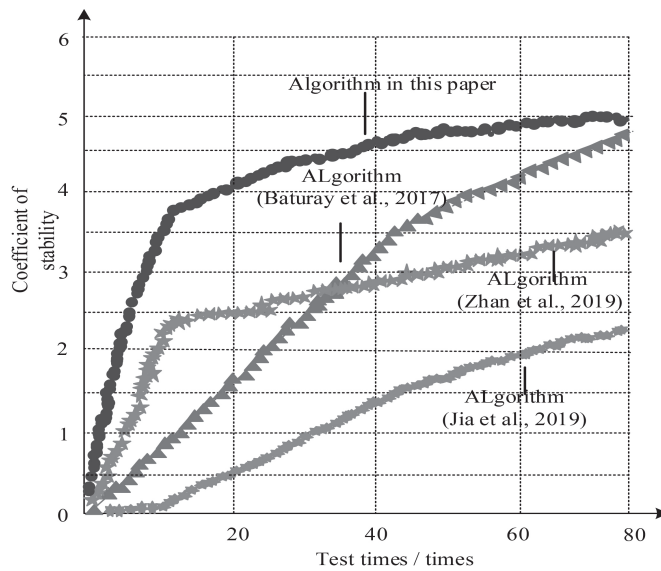
(a) Algorithm stability
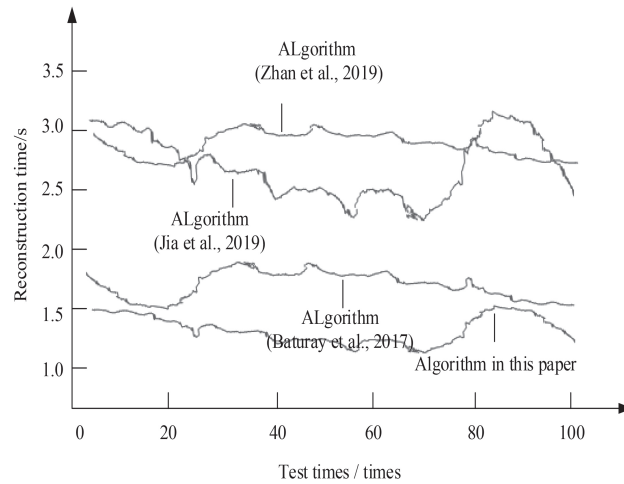
(b) Algorithm reconstruction time

Figure 4 Results for high-computing-power platform.

the decomposition coefficients of non-sparse natural signals under the transformation bases are mostly zero except for a small non-zero part. In addition to the sparse expression of coefficients, a measurement matrix should be designed to ensure that the data can be accurately reconstructed after effective compression sampling, so as to improve the stability of image reconstruction.

4. DISCUSSION

The interference multispectral compression sensing reconstruction technology can obtain a reconstructed image at a lower cost and does not require changing the hardware condition of the imaging equipment. Therefore, since it was proposed, interference multispectral compression and

perception reconstruction technology has become a research hotspot in the field of digital image processing, which has been comprehensively studied by scholars and research institutions. A large number of excellent methods have been proposed and applied to remote sensing imaging, medical imaging, multimedia communication, public security and other fields.

In this paper, machine learning is used to optimize the original reconstruction technology. The main work and innovations are discussed below.

In order to eliminate the reconstruction error of direct image processing, this paper proposes an image preprocessing module based on wavelet transform. There are obvious push sweep translation characteristics between the adjacent frames of the interference multispectral satellite image sequence. If the high-storage 3D wavelet transform is used directly, the translation characteristics are not used, and the image
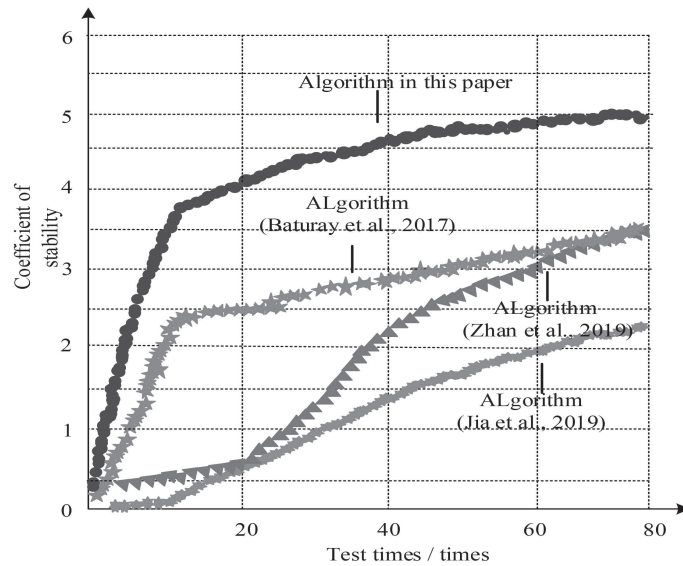
(a) Algorithm stability
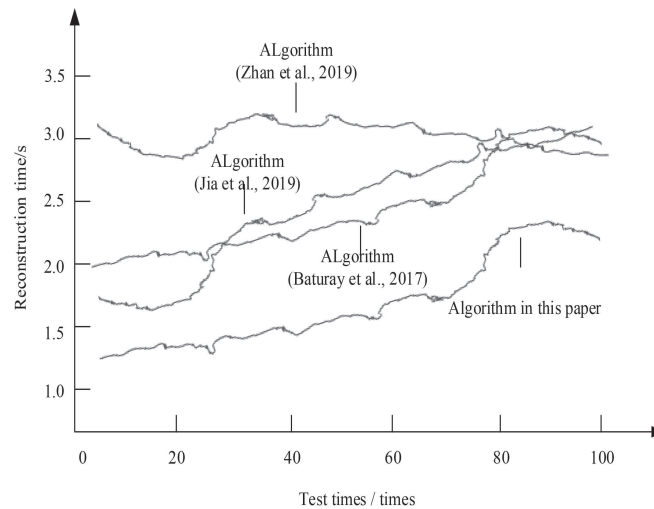
(b) Algorithm reconstruction time

Figure 5 Results of low-computing-power platform.

quality is not ideal. Therefore, it is necessary to study an algorithm which can make full use of the correlation of the image sequence and has low coding complexity. According to the characteristics of interference multispectral image and the requirements of the application environment, a new compression algorithm of interference multispectral image sequence is proposed. This algorithm does not need a three-dimensional wavelet transform; instead, it uses only the wavelet domain-matching algorithm to determine the difference image between two consecutive images. When coding the difference image, the system needs to store only two frames, which reduces the coding delay and power consumption. Moreover, the image quality is much better in comparison with the results obtained by direct single frame rate distortion optimized block code compression.

5. CONCLUSIONS

The existing reconstruction algorithms usually reconstruct high-resolution image blocks by weighting the high-resolution dictionary atoms according to a certain weight. In order to solve the above problems, in this paper, an interference multispectral image is designed based on machine learning according to the requirement analysis of image reconstruction algorithm in the practical application of a compressed sensing reconstruction algorithm. The test results show that the algorithm improves the deconstruction ability of the image block, and eliminates the blur and noise caused by interpolation by filtering the high-frequency information of the training image when training a low-resolution image, and improves the image reconstruction

effect. Using the compressed sensing theory and spectral imaging, the compressed sensing model is studied. The compressed sensing theory is applied to the processing of multispectral data and produces better results.

REFERENCES

1. Akagi, M., Nakamura, Y., Higaki, T., et al. 2019. Correction to: Deep learning reconstruction improves image quality of abdominal ultra-high-resolution CT. *European Radiology, 29*(8), 4526–4527.

2. Awasthi, N., Kalva, S.K., Pramanik, M., et al. 2018. Image-guided filtering for improving photoacoustic tomographic image reconstruction. *Journal of Biomedical Optics, 23*(9), 1–22.

3. Baturay, Ö., Duygu, Ö.T., Kaan, Ö.A., et al. 2017. Three-dimensional image reconstruction of macroscopic objects from a single digital hologram using stereo disparity. *Applied Optics, 56*(13), 84.

4. Bazulin, E.G., Sokolov, D.M. 2019. Reconstruction of ultrasound reflector images from incomplete data using the compressive sensing method. *Acoustical Physics, 65*(4), 432–443.

5. Cao, J., Wen, F.H. 2019. The impact of the cross-shareholding network on extreme price movements: Evidence from China. *Journal of Risk, 22*(2), 79–102.

6. Fayez M., Mandor M., El-Hadidy M., Bendary F. 2019. Fuzzy Logic Based Dynamic Braking Scheme for Stabilization of Inter -Area. *Acta Electronica Malaysia, 3*(2), 16–22.

7. Guo, L., 2021. Simulation of intelligent internet of things system based on machine learning and clustering algorithm. *International Journal of Engineering Intelligent Systems, 29*(6), 375–378.

8. Jia, T.T., Wang, J.H., Zheng, Y.Y., et al. 2019. Clique network super-resolution image reconstruction algorithm based on Laplace pyramid structure. *Journal of Chinese Computer Systems, 40*(8), 1760–1766.

9. Jung, H.G. 2017. Analysis of reduced-set construction using image reconstruction from a HOG feature vector. *IET Computer Vision, 11*(8), 725–732.

10. Min T., Jiansen Y., Ming W., Yuquan Z. 2019. Commercial Complex Intelligence and Program Research. *Information Management and Computer Science, 2*(1), 04–06.

11. Muggleton, S.H., Schmid, U., Zeller, C., et al. 2018. Ultra-strong machine learning: Comprehensibility of programs learned with ILP. *Machine Learning, 107*(7), 1119–1140.

12. Nalmpantis, C., Vrakas, D. 2019. Machine learning approaches for non-intrusive load monitoring: From qualitative to quantitative comparation. *Artificial Intelligence Review, 52*(1), 217–243.

13. Petersen, C.R., Prtljaga, N., Farries, M., et al. 2018. Mid-infrared multispectral tissue imaging using a chalcogenide fiber supercontinuum source. *Optics Letters, 43*(5), 999–1002.

14. Ramon, A.J., Yang, Y., Pretorius, P.H., et al. 2017. Investigation of dose reduction in cardiac perfusion SPECT via optimization and choice of the image reconstruction strategy. *Journal of Nuclear Cardiology, 25*(6), 1–12.

15. Rastogi S., Choudhary S. 2019. Face Recognition by Using Neural Network. *Acta Informatica Malaysia, 3*(2), 07–09.

16. Ren, Y.F., 2021. Noise filtering method of a 3D target image based on machine learning. *International Journal of Engineering Intelligent Systems, 29*(4), 195–204.

17. Wen, F., Xu, L., Chen, B., et al. 2019. Heterogeneous institutional investors, short selling and stock price crash risk: Evidence from China. *Emerging Markets Finance and Trade*, 1–14.

18. Wu, Q.Y., Sun, Y.F., Zhao, L. 2017. Depth image super-resolution reconstruction of the sparse representation and simulation. *Computer Simulation, 34*(5), 234–237.

19. Wu, Z., Ramsundar, B., Feinberg, E.N., et al. 2018. MoleculeNet: A benchmark for molecular machine learning. *Chemical Science, 9*(2), 513–530.

20. Zhan, Y.L., Chi, J., Ye, Y.N., et al.2019. Super resolution image reconstruction based on image similarity and feature combination. *Journal of Computer-Aided Design & Computer Graphics, 31*(6), 1018–1029.